LBL-32143
UC-401
Preprint

Lawrence Berkeley Laboratory
UNIVERSITY OF CALIFORNIA

CHEMICAL SCIENCES DIVISION

Submitted to Journal of Chemical Physics

Monte Carlo Simulations of Hydrophobic Weak Polyelectrolytes: Titration Properties and pH-Induced Structural Transitions for Polymers Containing Weak Electrolytes

A.P. Sassi, S. Beltrán, H.H. Hooper, H.W. Blanch,
J. Prausnitz, and R.A. Siegel

February 1992

Prepared for the U.S. Department of Energy under Contract Number DE-AC03-76SF00098

DISCLAIMER

LBL-32143

UC-401

Monte Carlo Simulations of Hydrophobic Weak Polyelectrolytes. Titration Properties and pH-Induced Structural Transitions for Polymers Containing Weak Electrolytes

Alexander P. Sassi, Sagrario Beltrán, Herbert H. Hooper**,*

*Harvey W. Blanch and John Prausnitz****

Department of Chemical Engineering

University of California

and

Chemical Sciences Division

Lawrence Berkeley Laboratory

1 Cyclotron Road

Berkeley, CA 94720

and

Ronald A. Siegel

Department of Pharmacy and Pharmaceutical Chemistry

University of California, San Francisco, CA 94143

This work was supported by the Director, Office of Energy Research, Office of Basic Energy Sciences, Chemical Sciences Division of the U.S. Department of Energy under Contract Number DE-AC03-76SF00098. Additional support was provided by the Whitaker Foundation.

*Present address: Departamento de Ingenería Química, Colegio Universitario de Burgos, Universidad de Valladolid, 09002 Burgos, Spain

**Present address: Air Products and Chemicals, Allentown, PA 18195

***To whom correspondence should be addressed.

MONTE CARLO SIMULATIONS OF HYDROPHOBIC WEAK POLYELECTROLYTES. TITRATION PROPERTIES AND pH-INDUCED STRUCTURAL TRANSITIONS FOR POLYMERS CONTAINING WEAK ELECTROLYTES

Alexander P. Sassi, Sagrario Beltrán, Herbert H. Hooper**,*

*Harvey W. Blanch and John Prausnitz****

Chemical Engineering Department, University of California

and

Chemical Sciences Division, Lawrence Berkeley Laboratory

Berkeley, CA 94720

and

Ronald A. Siegel

Department of Pharmacy and Pharmaceutical Chemistry

University of California, San Francisco, CA 94143

ABSTRACT

Monte Carlo simulation has been used to study titration and configurational properties of an isolated hydrophobic polymer containing weakly-ionizable groups. Using a cubic lattice, simulations were performed in the grand-canonical ensemble to include the effect of the local charge environment on the ionization of weak electrolyte segments. Properties were studied as a function of (1) polymer hydrophobicity, (2) fraction of ionizable segments, (3) solution ionic strength, and (4) pH. The polymer segments experienced three types of competing interaction: (1) excluded volume (2) attractive nearest-neighbor forces which account for the net balance of segment-segment, segment-solvent and solvent-solvent interactions, and (3) long-range electrostatic forces between ionized segments, calculated with a screened Debye-Hückel potential. Simulations show that the model chain expands with chain ionization, which depends on solution pH. As the chain becomes increasingly charged, the ionization process becomes more difficult because of rising local charge density around the ionizable segments. The effect of rising local charge density increases for larger fractions of ionizable groups, with increased hydrophobicity and with low ionic strength.

This work was supported by the Director, Office of Basic Energy Science, Chemical Sciences Division of the U.S. Department of Energy, under Contract Number DE-AC03-76SF0098.

* Present address: Departamento de Ingeniería Química, Colegio Universitario de Burgos, Universidad de Valladolid, 09002 Burgos, Spain

**Present address: Air Products and Chemicals, Allentown, PA 18195

***To whom correspondence should be addressed.

I. INTRODUCTION

Hydrophobic polymers and gels containing bound weak electrolytes undergo dramatic transitions in polymer structure (1-3) or gel volume (4) in response to changes in solution pH. At pH's where a large number of monomers are ionized, such polymers expand as polyelectrolytes; when the pH is such that few monomers are ionized, these polymers (or gels) collapse to condensed, hydrophobic conformations. The transformation from expanded to condensed conformations can be abrupt; some evidence suggests the existence of a discontinuous, two-state transition(5).

Several factors may contribute to structural transitions in hydrophobic polyelectrolytes and gels. Manning (6) suggested that the onset of counterion condensation (at a critical chain charge density) triggers polymer structural rearrangement. Schwarz and Siegel (7) have proposed a theory for pH-induced gel-volume collapse based on the composition dependence of the dielectric constant within the gel, and the resulting effect of gel volume on the Born energy of hydration.

In an earlier paper (8), we presented Monte Carlo simulations which indicate that structural transitions in hydrophobic, strong polyelectrolytes can result directly from the competition between coulombic repulsions and hydrophobic (segment-segment) attractions. In that work, large transitions were observed in the dimensions of a model polymer as the number of ionized groups on the chain increases; for highly hydrophobic chains, most of the change in structure occurred over a small range of chain ionization.

In the previous paper (8), variations in chain ionization were modeled by noting the effect of changes in polymer chemical composition, i.e., insertion or removal of permanently-ionized groups. While this can correspond to an experimentally realizable system, it is more common to observe the ionization and conformational behavior of polymers and gels containing weakly ionizable groups in response to variations in solution pH. In this paper we extend our earlier model (8) to treat polyelectrolyte titration. Thus, we consider polyelectrolytes where the number of potentially ionizable groups is constant, but where the degree of dissociation of these groups depends on solution pH. We perform simulations in the grand canonical ensemble (constant μ, V, T) to observe effects of local charge environments on the ionization of the chain.

In our simulations, we fix the pH and the intrinsic pK_o of the ionizable groups; the degree of ionization is allowed to find its equilibrium value. By performing

simulations over a range of pH, we obtain titration curves (the pH-dependence of the ionization). The resulting dependence of chain dimensions on degree of ionization is mapped onto a pH scale.

II. MODEL AND SIMULATION METHOD

The model and simulation method used in this work are similar to those described in Ref. 8. We discuss here the general model features and the differences between this work and Ref. 8. We are studying a model polymer chain at infinite dilution in a continuous solvent (water). The polymer is represented as a self-avoiding walk of N segments on a cubic lattice; each lattice location can contain only one polymer segment. In addition to excluded volume, the polymer segments experience short-range (non-electrostatic) and long-range (coulombic) interactions. A two-dimensional cross-section of our model is presented in Figure 1a. Non-bonded nearest-neighbor segments interact with a fixed potential ε; we investigate here (as in Ref. 8) $\varepsilon \leq 0$, i.e., the case where segment-segment contacts are either athermal or energetically favored over segment-solvent contacts. We consider the favorable segment-segment interaction to result from polymer hydrophobicity. Thus, our model polymer is analogous to a polyelectrolyte containing hydrophobic (e.g., hydrocarbon) groups. The hydrophobic groups tend to collapse the polymer, while the ionized groups tend to expand the chain; the net result is a rich set of configurational properties, varying from collapsed to expanded structures, depending on system conditions (8).

Ionized segments on the chain interact through screened coulombic repulsions. In Ref. 8, segments were either completely ionized (with a valence of unity) or uncharged. Ionized segments were evenly spaced along the chain, and the fraction of the total segments carrying charge, λ, varied from 0 to 1.0. In that work, changes in λ correspond to variations in polymer composition; i.e., a series of chains with different λ is the same as a series of copolymers containing different ratios of charged to uncharged monomer. In Ref. 8, the charged monomers are strong electrolytes because their degree of dissociation is independent of solution conditions.

In this work we consider the effect of pH on the behavior of a polymers containing weak electrolytes. We now define λ as the fraction of segments which are *potentially* ionizable. We define α as the ionization, i.e., the fraction of these

segments which is dissociated. Considering the weakly ionizable groups to be basic (for example, an amine), the chemical equilibrium of interest for a single segment is:

$$NH^+ \leftrightarrow N + H^+ \tag{1}$$

where NH^+ is the protonated segment. At any stage of the titration, we can define a dissociation constant, K_a, by:

$$\frac{[NH^+]}{[N]} = \frac{[H^+]}{K_a} \tag{2}$$

where [ ] denotes monomolar concentration, the activity coefficients all being assumed to be unity. Generally, K_a will depend on the degree of charge on the polyelectrolyte, α:

$$\alpha = \frac{[NH^+]}{[N] + [NH^+]} \tag{3}$$

because of electrostatic interaction between ionizable groups. Therefore, it is also useful to define an *intrinsic* dissociation constant, K_o, which is the value that K_a would take in the absence of interaction between charge groups. (K_o can be interpreted as the limiting value of K_a as α approaches zero, or as the dissociation constant observed in a dilute monomeric solution of the ionizable component) The "true" equilibrium constant, K_a, of each group on the model chain will be determined by the local charge environment, i.e., by the number and spatial arrangement of nearby charges.

When $\alpha=0$, all ionizable segments on the polymer are uncharged, and we reach the well-studied limit of an attractive self-avoiding walk. When $\alpha=1$, all ionizable segments (i.e., the fraction λ of the total number of segments) are charged, and we obtain the limit studied in Ref. 8. By varying pH, we consider conditions between those two limits.

Since we desire to determine the degree of ionization and the configuration of a polymer chain at a given pH, simulations in the grand canonical ensemble are appropriate (constant μ_{H^+}, V, T; where $\mu_{H^+} = \mu^\circ_{H^+} - 2.3RTpH$). In simulations in the grand canonical ensemble, the ionization α fluctuates; therefore, the energetics of

protonating or deprotonating an ionizable segment depend on the local environment surrounding that group.

In the grand canonical simulation, we fix the pH and the intrinsic K_O at the beginning of the simulation. Ionizable segments are either completely ionized (protonated) or uncharged. In 10% of the simulation steps (10% chosen to optimize simulation time), one of the potentially ionizable segments is chosen at random. If the selected segment is neutral, the segment becomes ionized, and vice-versa. In this manner, the ionization of the chain, α, is allowed to fluctuate and thereby reach an equilibrium value.

The configurational energy for the chain is a sum of electrostatic and non-electrostatic (dispersion-force) contributions:

$$E = E_{el} + E_{nel} \tag{4}$$

The non-electrostatic energy is

$$E_{nel} = \varepsilon m \tag{5}$$

where m is the total number of contacts between non-bonded nearest neighbor segments. The electrostatic energy is the sum over long-range coulombic interactions between all pairs of ionized segments:

$$E_{el} = \sum_{i}^{N-1} \sum_{j=i+1}^{N} u_{ij} \tag{6}$$

where N is the number of segments in the chain and u_{ij} is given by a screened Debye-Hückel coulombic potential (8):

$$u_{ij} = \frac{q_i\, q_j}{D\, r_{ij}} \exp(-\kappa r_{ij}) \tag{7}$$

where segments i and j carry charge q_i and q_j, respectively, and are separated by a distance r_{ij}. The dielectric constant D is that of water at 25°C. The charges on segments i and j are determined as described above. The inverse Debye screening length, κ, is given by (9):

$$\kappa = \left[\frac{4 \pi e^2 N_A \sum_i z_i C_i}{D k T} \right]^{\frac{1}{2}} \tag{8}$$

where e is the electron charge, N_A is Avogadro's number, z_i is the valency of the ionic species i, C_i is the concentration of ionic species i, D is the dielectric constant for pure water at 25 C, k is Boltzmann's constant, and T is the temperature.

We consider the polyelectrolyte at infinite dilution; thus, the sum in Eqn. (8) is over the species of *added* electrolyte, and does not include the charges on the polymer or the counterions. For convenience, in the discussion of results we assume that the added electrolyte is a 1:1 salt, and we refer either to the Debye screening length, κ^{-1}, or to the concentration of added electrolyte (C_i) which produces in that screening length.

Polyelectrolyte configurational properties were calculated using the Metropolis Monte-Carlo method (10). The chain is initially placed in a three-dimensional staircase configuration; successive configurations are generated by combination of elementary chain movements.

We found that when we used the algorithm for chain motion as described in Ref. 8 (a combination of reptation and internal movements) in the grand canonical ensemble, the number of chain movements required to reach equilibrium increased probihitively. To decrease computational time, we used an algorithm described by Valleau (11) to generate successive configurations. The segment adjacent to one of the end segments is pinned on the lattice; its position does not change. Reptation moves are no longer used. The other types of moves (end-flip, kink-jump, crankshaft) are performed as before (8) and are illustrated in Figure 1b. When using this algorithm to generate successive configurations, we obtain the same results for uncharged chains as those published in Ref. 12, and the same relationship between ionization and end-to-end distance as that in Ref. 8. In the grand canonical ensemble, new configurations are accepted based on the probability (for a weak base):

$$p_{s+1} = min\{1, exp[(-\Delta E/kT) + \Delta m_c(pK_o - pH) ln 10]\} \tag{9}$$

where ΔE is the energy change [c.f. Eqs. (4)-(6)] in going from configuration s to configuration $s+1$, Δm_C is the change in number of ionized segments from s to $s+1$, and $pK_O = -log_{10}(K_O)$. In Equation (9), the statistical weights have been decoupled

for changes in energy due to configuration $\{exp(-\Delta E/kT)\}$ and for those due to protonation/deprotonation $\{exp[\Delta m_c(pK_o-pH)ln10]\}$.

The chain is initially relaxed through $5x10^4$ attempted movements (cycles); configurational properties are calculated (and recorded) every $3x10^4$ cycles. This sampling frequency was found sufficient to generate statistically uncorrelated configurations for the 40-segment chains studied here. A total of 900 configurations are sampled for each run, requiring $2.7x10^7$ Monte-Carlo cycles. The property of primary interest (with regard to conformation) here is the size of the polymer coil, characterized by its mean-square end-to-end distance:

$$\langle r^2 \rangle = \langle (r_N - r_1)^2 \rangle \tag{10}$$

where r_1 and r_N are the position vectors locating the first and last chain segment, respectively, and $\langle\ \rangle$ denotes an average over the 900 samples in a Monte-Carlo run. Coil size is reported here as a reduced variable; $\langle r^2 \rangle$ is reduced by the value it would have in a fully extended configuration, $(N-1)^2 l^2$, where l is the lattice length. (We also calculated the mean square radius of gyration and found that it follows the same trends as $\langle r^2 \rangle$ with respect to hydrophobicity (ε/kT), ionic strength (κ^{-1}), pH and fraction of ionizable groups (λ). Those results are not presented here.)

In order to study the effect of the local charge environment on the average pK_a ($pK_a = -\log_{10}[K_a]$), we define the variable $\Delta pK_a = pK_a - pK_o$. By a straightforward rearrangement of the Henderson-Hasselbach equation (13), we have the following:

$$\Delta pK_a = pH - pK_o + \log_{10}\left(\frac{\alpha}{1-\alpha}\right) \tag{11}$$

If the titration curve (relation between ionization and pH) follows the Langmuir isotherm (Eqn. 2), ΔpK_a is zero. Thus, the variable ΔpK_a is a measure of the deviation in pK_a of the ionizable segments from the intrinsic pK_o. The larger the magnitude of ΔpK_a, the greater the interaction between the charged groups.

III. RESULTS AND DISCUSSION

Configurational properties were calculated for 40-segment chains as a function of pH, polymer hydrophobicity (ε/kT), fraction of ionizable segments (λ), and the Debye screening length, (κ^{-1}). We observed in Ref. 8 the qualitative behavior of model polyelectrolytes with competing hydrophobic and coulombic interactions and

found evidence for a structural transition induced by increasing chain ionization. Our goal here is to illustrate the effect of making the ionization of the polymer sensitive to pH and charge-charge interactions; therefore, we replace the charged segments of Ref. 8 with weakly-ionizable segments. Our model polymer is thus equivalent to a copolymer containing a hydrophobic monomer and a weakly basic monomer. In essence, our model provides a simplified representation of a short polypeptide.

Because our simulations are for a single polyelectrolyte chain at infinite dilution, we consider only intra-chain interactions and neglect energetic contributions from inter-chain electrostatics or network elasticity as found in typical polymer solutions or gels. However, with our model, we expect to observe the same qualitative trends in chain conformation as those that occur in dilute solutions, where interchain electrostatics are not significant.

Because the ionizable segments are weakly basic, these segments are charged at pH's much lower than pK_o and uncharged at pH's higher than pK_o. Thus, the chain expands at low pH, and condenses to a more compact configuration at high pH. In the Langmuir case (no interactions between charged groups), the transformation between the two regimes is sharp (though continuous) and is centered around the pK_o.

Experimentally, the K_a of any individual ionizable group depends on the electrical field surrounding that group. As the ionic strength and the number and proximity of surrounding charges changes, the local electrical field changes, altering K_a. In the grand canonical ensemble, since the ionization α is allowed to change freely at a given pH, the K_a of an ionizable group is determined by its local charge environment. Figure 2 presents the titration curves obtained from simulation in the grand canonical ensemble for a chain with λ =0.325 and ε/kT = 0 and -1 in solution of ionic strength 0.001 M ($\kappa^{-1}=96.2\text{Å}$). For reference, the titration curve calculated assuming no electrostatic interactions is also shown (i.e., pure Langmuir case). The titration curves obtained from simulation differ significantly from the pure Langmuir case.

If, as we would expect, the conformation of the model polymer of fixed hydrophobicity and number of charges is not dependent on the model by which the charge state is attained (path independent), then mapping of the mean square end-to-end distance against the ionization of the chain should be equivalent in Ref. 8 and in the grand canonical simulations performed here. This is indeed the case as illustrated in Figure 3, which shows the dependence of end-to-end distance on

ionization for Reference 8 and the grand canonical simulation for $\lambda = 0.325$, $\varepsilon/kT = -1$ and $\kappa^{-1}=96.2\text{Å}$.

Superposition of the data in Figure 2 implies that, if the titration behavior of the model polyelectrolyte is known for a given set of conditions, the pH-dependence of conformational parameters can be obtained from simulations of the type in Reference 8. Effectively, then, the conformation of the chain is uncoupled from the titration curve; for a given state of ionization, the polyelectrolyte adopts a certain average conformation. However, the titration curve is not uncoupled from the conformational state of the chain, and thus cannot be obtained from a simulation like that of Reference 8. If the titration curve is not known a priori, then the simulation must be performed in the grand canonical ensemble.

We now discuss results of sets of simulations which were designed to explore the effect of different parameters on titration and configurational behavior. In the first set of simulations, we consider a series of chains in a 0.1 M solution ($\kappa^{-1}=9.62\text{Å}$) with constant hydrophobicity (ε/kT = -1) and varying fraction of ionizable groups (λ). Figure 4a shows the deviation ΔpK_a as defined in Equation 11 plotted against the ionization α of the chain. In general, the magnitude of ΔpK_a increases with rising ionization, implying that as the chain becomes increasingly charged, it becomes increasingly difficult to ionize a segment on that chain. As λ increases, the magnitude of ΔpK_a also increases since the charges are all confined to the same chain. While at low values of λ (10%), the relationship between ΔpK_a and α is virtually linear, a significant change in slope occurs for cases where $\lambda > 0.325$. Considering the data for λ=0.325, the deviation ΔpK_a is relatively independent of the ionization for α>0.6.

We believe that this independence is a result of the onset of chain expansion; the chain now expands with the ionization of segments to such an extent that the difficulty of charging a segment remains nearly constant. Figure 4b shows both the mean square end-to-end distance and as a function of $pH\text{-}pK_o$. for the case λ=0.325 of Figure 4a. We note that the inflection points of each curve do indeed occur at nearly the same pH; that is, the deviation ΔpK_a becomes independent of α as the chain starts to expand.

Figure 4c shows the pH-induced transitions in the mean square end-to-end distance for the same simulations as those in Figure 4a. We note the absence of chain expansion for the case λ = 0.1. The transitions are distinct and gradual, reminiscent of acid-induced protein-denaturation curves (14). As expected from the observations in Ref. 8, the degree of expansion of the chain is larger for higher values of λ.

In the second set of simulations, we consider a series of chains with constant hydrophobicity ($\varepsilon/kT=-1$) and fraction of ionizable groups ($\lambda=0.325$) in solutions of varying ionic strength ($96.2\text{Å} \leq \kappa^{-1} \leq 3.04\text{Å}$). As in Figure 4a, Figure 5a presents the dependence of the deviation ΔpK_a on ionization. Again, we observe that as the chain is ionized, it becomes increasingly difficult to protonate the remaining groups. The presence of added ions acts to shield charges on the chain from each other; therefore, as ionic strength increases, the ionizable groups act more independently, and the magnitude of ΔpK_a decreases. This decrease in magnitude of ΔpK_a with ionic strength is in qualitative accord with theoretical predictions by Katchalsky (15). Because charges on the chain are more effectively screened from each other at high salt concentration, thus the energetic penalty for ionizing a segment is smaller. The analogous effect of NaCl concentration on the titration curves of alternating maleic anhydride/styrene copolymers was observed by Ohno et al. (16), on those for maleic acid/alkyl vinyl ether copolymers by Dubin and Strauss (1).

The pH-induced transitions in the mean square end-to-end distance for the second set of simulations are shown in Figure 5b. In accord with the observations in Ref. 8, the charge-shielding at higher ionic strength causes the magnitude of the transition to become smaller.

In the final set of simulations, we varied the hydrophobicity of the segments for a chain with λ = 0.325 in a 0.1 M solution. Figure 6a illustrates the effect of increasing hydrophobicity on the relation between ΔpK_a and α. Included in Figure 6a are simulation data for a chain with no attractive neighbor-neighbor interactions (ε/kT = 0). The dependence of ΔpK_a on α when ε/kT =0 is approximately linear. As the strength of the neighbor-neighbor interactions increases, ΔpK_a becomes more negative. This increase in the magnitude of ΔpK_a with more attractive short-range interactions can be understood upon consideration of the effect of hydrophobicity on chain conformation. The stronger the attractive interactions between segments, the tighter the chain becomes, bringing ionizable segments closer together. This, in turn, increases the local charge density, making it more difficult to ionize groups. Dubin and Strauss also observed an increase in pK_a (analogous to our decrease in pK_a for a weak-base-containing polyelectrolyte) for maleic acid/alkyl vinyl ether copolymers in 0.1M NaCl when the comonomer was changed from ethyl vinyl ether to the more hydrophobic butyl vinyl ether (1).

An increase in the strength of neighbor-neighbor attraction introduces curvature into the relation between ΔpK_a and α. For the most hydrophobic chain studied (ε/kT=-1.5), the dependence of ΔpK_a on α shows an inflection point,

indicating that (over a small range of α) the chain rearranges such that it becomes relatively easier to charge the n+1th charge relative to the nth charge. Experimentally, Dubin and Strauss have observed an inflection point in the titration of maleic anhydride/butyl vinyl ether copolymers (1). We stress that deviations from a linear relationship between ΔpK_a and α are entirely due to the hydrophobicity of the chains.

The results in Figure 6b show the effect of hydrophobicity on the pH-induced transitions for the same simulations as those in Figure 6a. Again, we show the case where there are no attractive neighbor-neighbor interactions. As the neighbor-neighbor attraction becomes stronger, the chains are more compact, and the magnitude of the transition decreases. We also see a dramatic shift in the pH at which the transition occurs. As the hydrophobicity increases, the transition shifts to more acidic pH, as it becomes more difficult to protonate the chain.

Our simulations may be contrasted with simulation results reported by Reed and Reed (17), who studied the electrostatic persistence length and radius of gyration of off-lattice chains where all segments were weak electrolytes. Reed and Reed's simulations were also performed in the grand canonical ensemble, but do not include short-range interactions between segments. Our earlier work (8) on lattice-bound copolymers of fixed ionization provides a basis for examining the effect of competing hydrophobic (short-range) and electrostatic (long-range) interactions on polymer configurational properties. In that work, we found evidence for the occurrence of charge-induced structural transitions in hydrophobic polyelectrolytes. In this work, we also study lattice-bound copolymers with electrostatic and short-range interactions, but in the grand canonical ensemble where the ionization is not fixed. Thus, the study reported here investigates such transitions in a manner more directly analogous to those observed experimentally.

While we have captured the main features of pH-induced transitions with our model, we have neglected several experimental phenomenon in our simulations for simplicity. For example, we assume that pK_o is independent of ionic strength, although, experimentally, K_o is known to be weakly-dependent on ionic strength (18). Additionally, we assume the dielectric constant, D, to be invariant in the screened coulombic potential. Realistically, the dielectric constant between two ionized segments will be a function of the local segment density (19). Finally, we assume ε to be constant. However, this neglects the possibility that ε depends on charge state, since ionization of an amine group makes it more polar.

In addition to providing information about the configuration and state of ionization of the model chain, our simulation data can be used to calculate binding energies (ΔG_b) for the model polyelectrolyte. Schellman (20) showed that the differential binding energy of a ligand is given by

$$d\Delta G_b = -RT\{d[\ln(a)]\} \tag{12}$$

where R is the universal gas constant, T is the temperature, r is the average number of hydrogen ions bound and a is activity of the free ligand in solution. By expressing a in terms of pH and r as the product $\alpha\lambda N$ (for our simulations), we have:

$$\Delta G_b = -2.303\lambda NRT\int_{-\infty}^{pH} \alpha d(pH) \tag{13}$$

The above integral can be evaluated numerically from the titration curve. For the Langmuir case ($\Delta pK_a = 0$), the integral can be evaluated analytically to give the following:

$$\Delta G_b = -2.303\lambda NRT\ln[1 + 10^{\,pKa-pH}] \tag{14}$$

As an example, we have evaluated Eqn. 14 for our simulation results for the cases $\lambda=0.325$, $\kappa^{-1}=9.62\text{Å}$ and $\varepsilon/kT = 0$ and -1. The binding energy ΔG_b as a function of $pH-pK_o$ thus obtained is compared to Eqn. 14 in Figure 10. As we expect, the binding energy for the Langmuir case is significantly more negative than that when interactions between the charged groups are taken into account. The binding energies are also more negative in the absence of hydrophobicity which tends to hold the charges in greater proximity.

IV. CONCLUSIONS

Ionization and configurational properties were calculated by Monte Carlo simulations for a model polymer at infinite dilution as a function of pH, polymer hydrophobicity (ε/kT), fraction of ionizable segments (λ), and ionic strength(κ^{-1}). The polymer was represented on a cubic lattice by a 40-segment chain containing hydrophobic and weakly-basic segments, characterized by an intrinsic pK_o. Along with excluded volume, the polymer segments experienced two other competing interactions: (1) intramolecular electrostatic interaction between ionized segments, calculated with a screened Debye-Hückel potential, and (2) non-electrostatic forces, represented by the potential ε; this potential accounts for short-range segment-segment, segment-solvent and solvent-solvent interactions. Our model represents the main features of pH-sensitive, hydrophobic polyelectrolyte behavior at infinite

dilution. Simulation in the grand canonical ensemble showed the presence of pH-induced transitions in chain conformation as a result of chain ionization. Predictions of the influence of chain hydrophobicity, ionic strength, and fraction of ionizable segments on titration properties of the model polyelectrolyte are in accord with experimental observations.

ACKNOWLEDGMENTS

This work was supported by the Director, Office of Energy Research, Office of Basic Energy Sciences, Chemical Sciences Division of the U.S. Department of Energy under contract No. DE-AC03-76SF00098 and by a grant from the Whitaker Foundation. A.S. is grateful to the National Science Foundation for a pre-doctoral fellowship, and S.B. is grateful to the Spanish Ministry of Education and Science (MEC) for a post-doctoral fellowship. The calculations reported here were performed on the IBM 3090 at the U.C. Berkeley Computing Center; we acknowledge with thanks the generous computation time provided by the Computing Center. The authors are grateful to David Chandler, Dirk Stigter and Doros Theodorou for helpful comments and suggestions.

FIGURE CAPTIONS:

Figure 1. (a) Two-dimensional cross-section of the model chain illustrating attractive short-range interactions (ε) between non-bonded, nearest neighbors and electrostatic interactions between charged segments (u_{ij}). Lattice positions are marked by circles (segments). (b) The three types of attempted chain motions.

Initial configurations are denoted by filled circles (segments) joined by solid lines (bonds); new configurations are denoted by open circles and dashed lines. (a) When the randomly selected bead (bead i) is an end segment, the terminal bond can rotate or flip to place this bead in a neighboring site; (b) When bead i is joined by two 90° bonds, and the lattice site opposite i is not filled by segment $i+2$ or segment $i-2$, the attempted move is a two-bond flip to place i in this opposite lattice site; (c) When bead i is joined by two 90° bonds ant the site opposite i is filled by segment $i+2$ or segment $i-2$, the attempted move is a three-bond crankshaft rotation to place bead i and a neighboring bead in either of the two locations above or flip the two beads 180°.

Figure 2. Titration curves based on the Langmuir case (closed circles) and from Monte Carlo simulation for a 40-bead chain ($\lambda=0.325$, $\kappa^{-1}=96.2\text{Å}$, $\varepsilon/kT=0$ *(circles)*, -1 *(squares)*).

Figure 3. Mapping of the normalized mean-square end-to-end distance against chain ionization for $\varepsilon/kT=-1$, $\kappa^{-1}=96.2\text{Å}$ and $\lambda=0.325$. Data from Ref. 8 are marked by closed circles; those from this work by open circles.

Figure 4. (a) Dependence of ΔpK_a on ionization, α, for chains with constant hydrophobicity $(\varepsilon/kT=-1)$ in 0.1 M ionic strength solution $(\kappa^{-1}=9.62\text{Å})$ and variable fraction of ionizable groups $(0.1\leq\lambda\leq0.5)$. (b) Dependence of ΔpK_a and the reduced end-to-end distance on $pH-pK_o$ for $\varepsilon/kT=-1$, $\lambda=0.325$ and $\kappa^{-1}=9.62\text{Å}$. Triangles denote ΔpK_a , and squares denote end-to-end distance. (c) Dependence of the reduced end-to-end distance on $pH-pK_o$ for chains with constant hydrophobicity $(\varepsilon/kT=-1)$ in 0.1M ionic strength solution $(\kappa^{-1}=9.62\text{Å})$ and variable fraction of ionizable groups $(0.1\leq\lambda\leq0.5)$.

Figure 5. (a) Dependence of ΔpK_a on ionization for chains with constant hydrophobicity $(\varepsilon/kT=-1)$ and fraction of ionizable groups $(\lambda=0.325)$ in solutions of different ionic strengths $(96.2\text{Å}\leq\kappa^{-1}\leq3.04\text{Å})$. (b) Dependence of the reduced end-to-end distance on $pH-pK_o$ for chains with constant hydrophobicity $(\varepsilon/kT=-1)$ and fraction of ionizable groups $(\lambda=0.325)$ in solutions of different ionic strengths $(96.2\text{Å}\leq\kappa^{-1}\leq3.04\text{Å})$.

Figure 6. (a) Dependence of ΔpK_a on ionization as a function of chain hydrophobicity $(-1.5\leq\varepsilon/kT\leq0)$ for chains with a constant fraction of ionizable groups

in 0.1M ionic strength solution($\kappa^{-1}=9.62\text{Å}$). (b) Dependence of the reduced end-to-end distance on $pH-pK_o$ as a function of chain hydrophobicity ($-1.5\leq\varepsilon/kT\leq 0$) for chains with a constant fraction of ionizable groups in 0.1M ionic strength solution($\kappa^{-1}=9.62\text{Å}$).

Figure 7. Dependence of binding energy ΔG_b on $pH-pK_o$ for the Langmuir case (closed circles) and for our simulations ($\lambda=0.325$, $\kappa^{-1}=9.62\text{Å}$, $\varepsilon/kT=0$ *(open circles)*, -1 *(open squares)*).

REFERENCES

1. P. L. Dubin and U. P. Strauss, J. Phys. Chem., 74, 2842 (1970).
2. U. P. Strauss, B. W. Barbieri and G. Wong, J. Phys. Chem. 83, 2840 (1979).
3. U. P. Strauss, Macromolecules 15, 1576 (1982).
4. R. A. Siegel and B. A. Firestone, Macromolecules 21, 5324 (1988).
5. E. S. Matsuo and T. Tanaka, J. Chem. Phys., 89, 1695 (1988).
6. G. S. Manning, J. Phys. Chem. 89, 3772 (1988).
7. B. Schwarz and R. A. Siegel, work in preparation.
8. H. H. Hooper, S. Beltran, A. P. Sassi, H. W. Blanch and J. M. Prausnitz, J. Chem. Phys. 93, 2715 (1990).
9. P. H. Rieger, *Electrochemistry* (Prentice-Hall, Inc., 1987).
10. N. Metropolis, A. W. Rosenbluth, M. N. Rosenbluth, A. H. Teller and E. Teller, J. Chem. Phys. 21, 1087 (1953).
11. J. P. Valleau, Chem. Phys., 129, 163 (1989).
12. H. H. Hooper, H. W. Blanch and J. M. Prausnitz, Macromolecules, 23, 4820 (1990).
13. L. Stryer, *Biochemistry* (W.H. Freeman, Inc., 1981).
14. B. T. Nali and K. A. Dill, ed., *Conformations and Forces in Protein Folding* (American Association for the Advancement of Science, 1991).
15. A. Katchalsky, N. Shavit, and H. Eisenberg, J. Polym. Sci., 13, 69 (1954).
16. N. Ohno, K. Nitta, S. Makino and S. Sugai, J. Polym. Sci. 11, 413 (1973).
17. C. Reed and W. Reed, J. Chem. Phys. 94, 8479 (1991).
18. F. Mandel, Eur. Polym. J., 6, 807 (1970).
19. C. Tanford, *Physical Chemistry of Macromolecules* (John Wiley and Sons, 1961).
20. J. Schellman, Biopolymers, 14, 999 (1975).

Figure 1A

MODEL POLYELECTROLYTE CROSS-SECTION

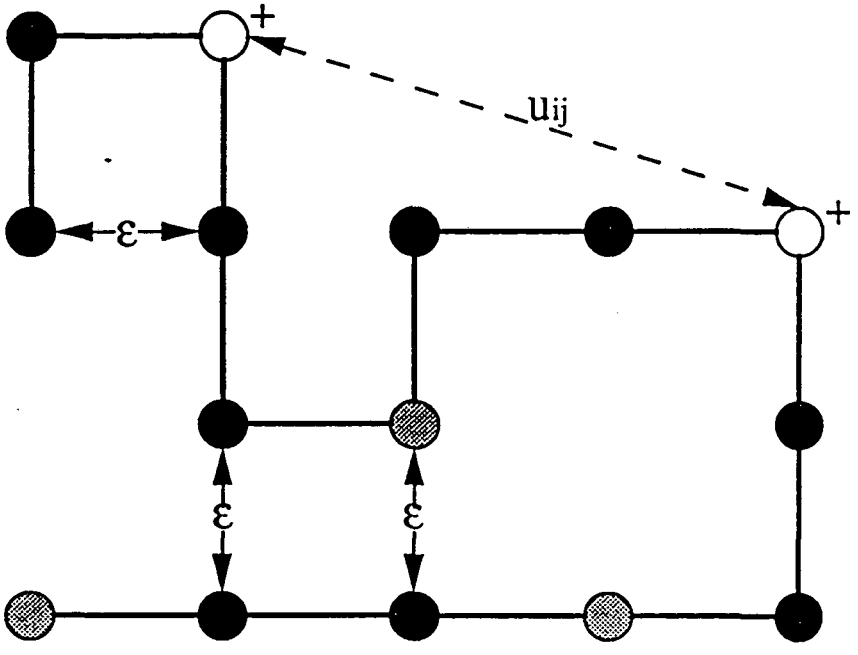

○ potentially ionizable bead (charged)

◌ potentially ionizable bead (uncharged)

● nonionizable bead

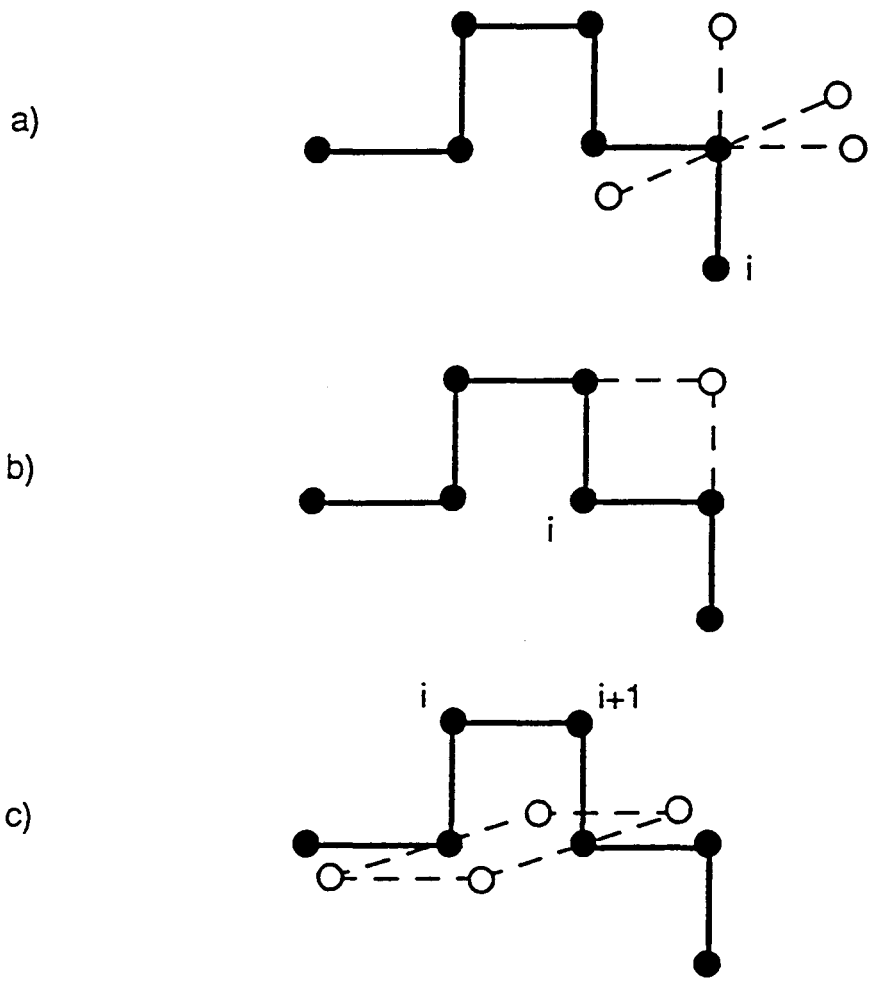

Figure 1 B

Figure 2

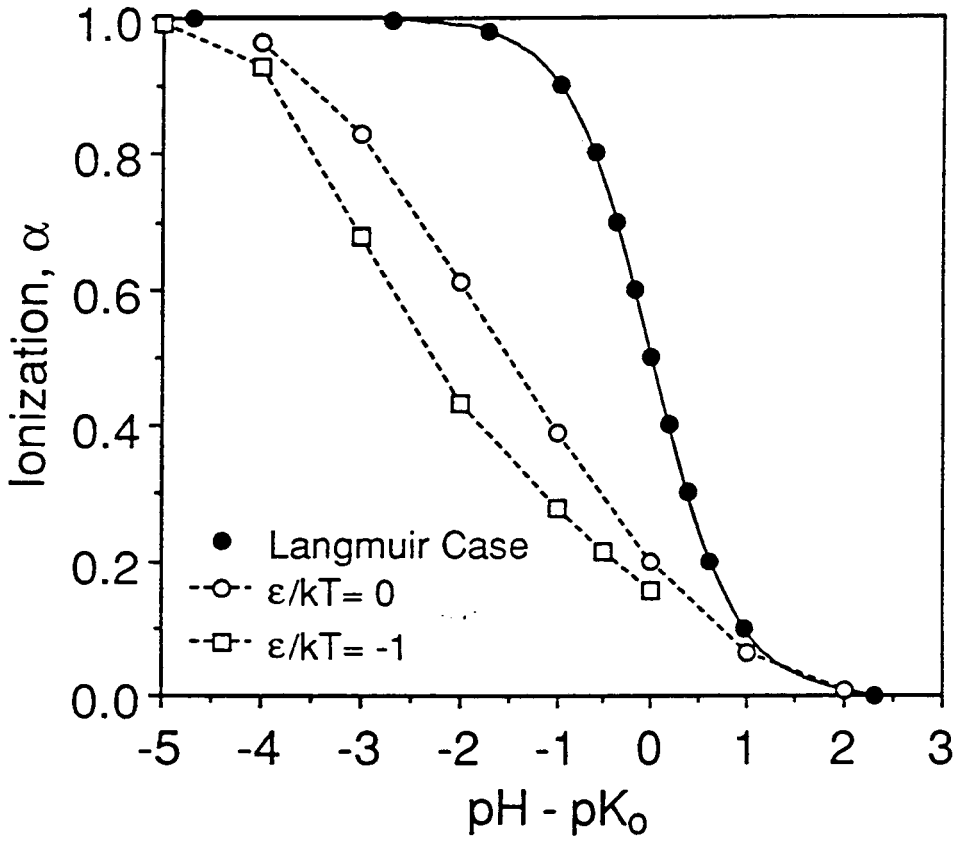
1.0
0.8
0.6
0.4
0.2
0.0
Ionization, α
Langmuir Case
ε/kT= 0
ε/kT= -1
-5
-4
-3
-2
-1
0
1
2
3
pH - pK$_o$

Figure 3

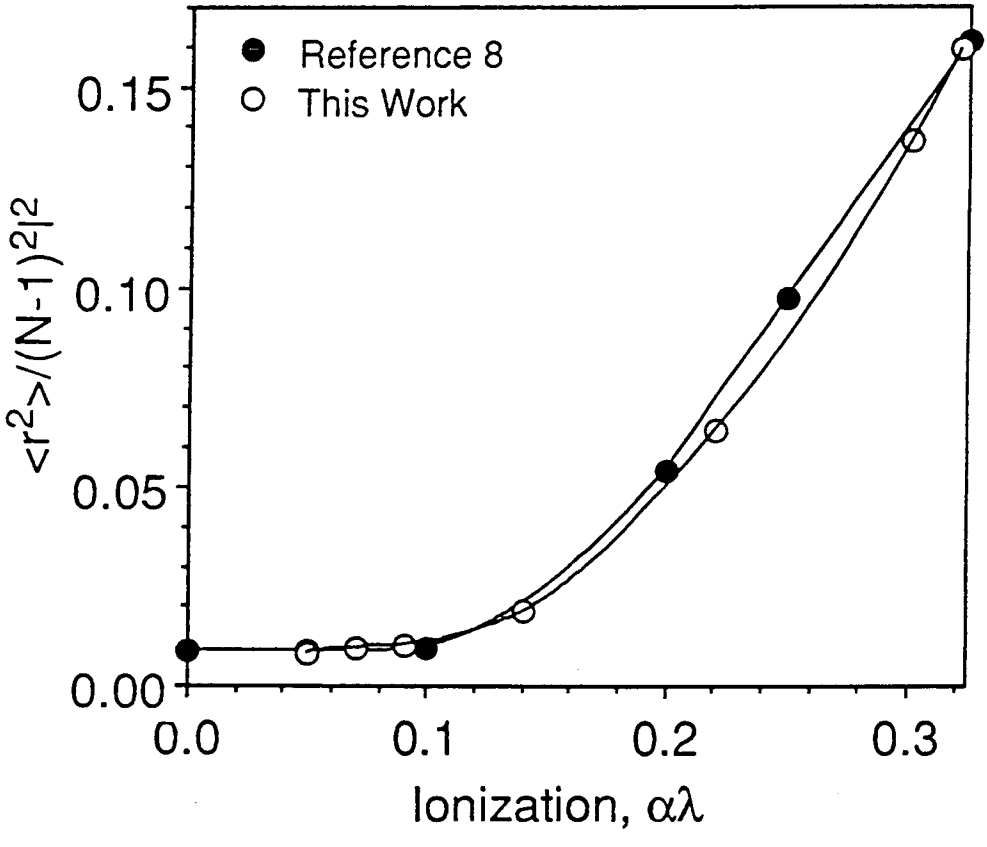
Reference 8
This Work
0.15
0.10
0.05
0.00
$\langle r^2 \rangle / (N-1)^2 I^2$
0.0
0.1
0.2
0.3
Ionization, $\alpha\lambda$

Figure 4A

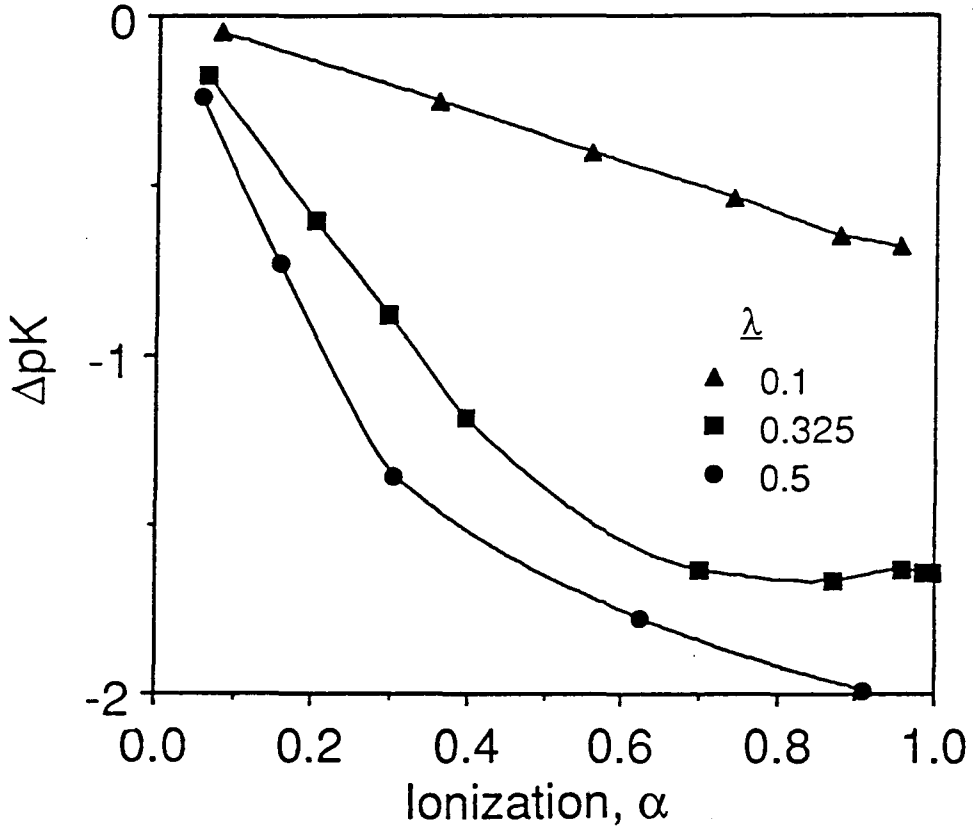

Figure 4B

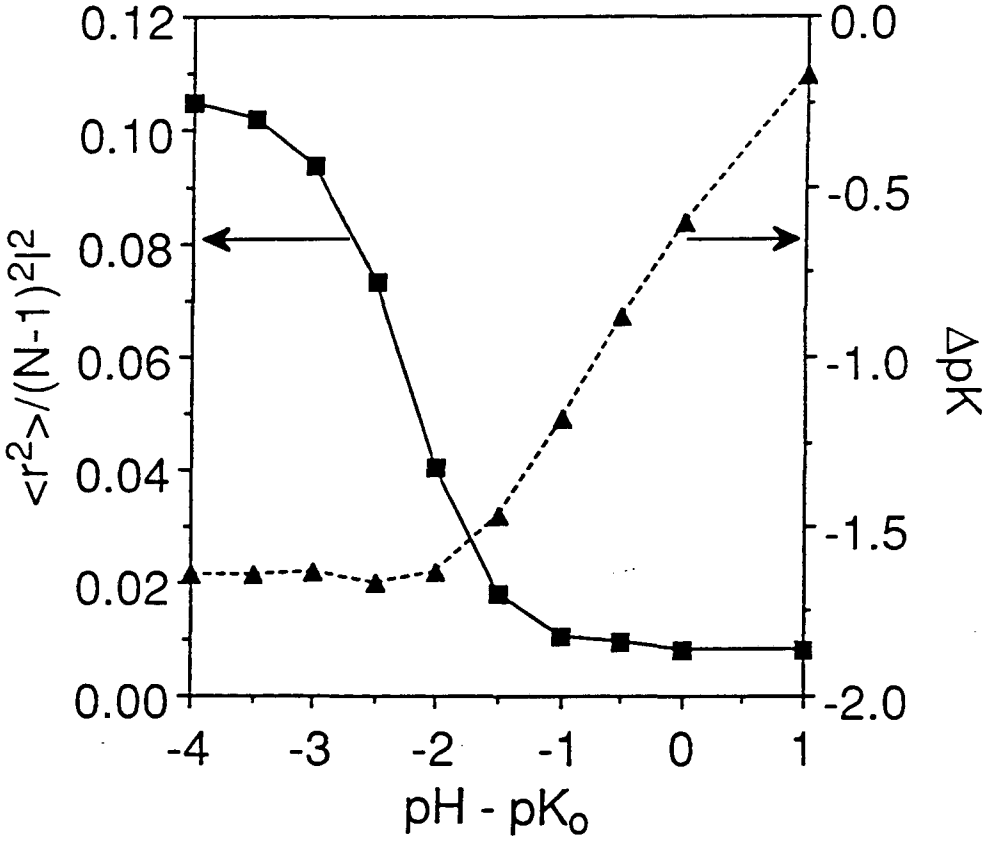
0.12
0.10
0.08
0.06
0.04
0.02
0.00
0.0
-0.5
-1.0
-1.5
-2.0
-4
-3
-2
-1
0
1
$\langle r^2 \rangle / (N-1)^2 l^2$
ΔpK
$pH - pK_o$

Figure 4C

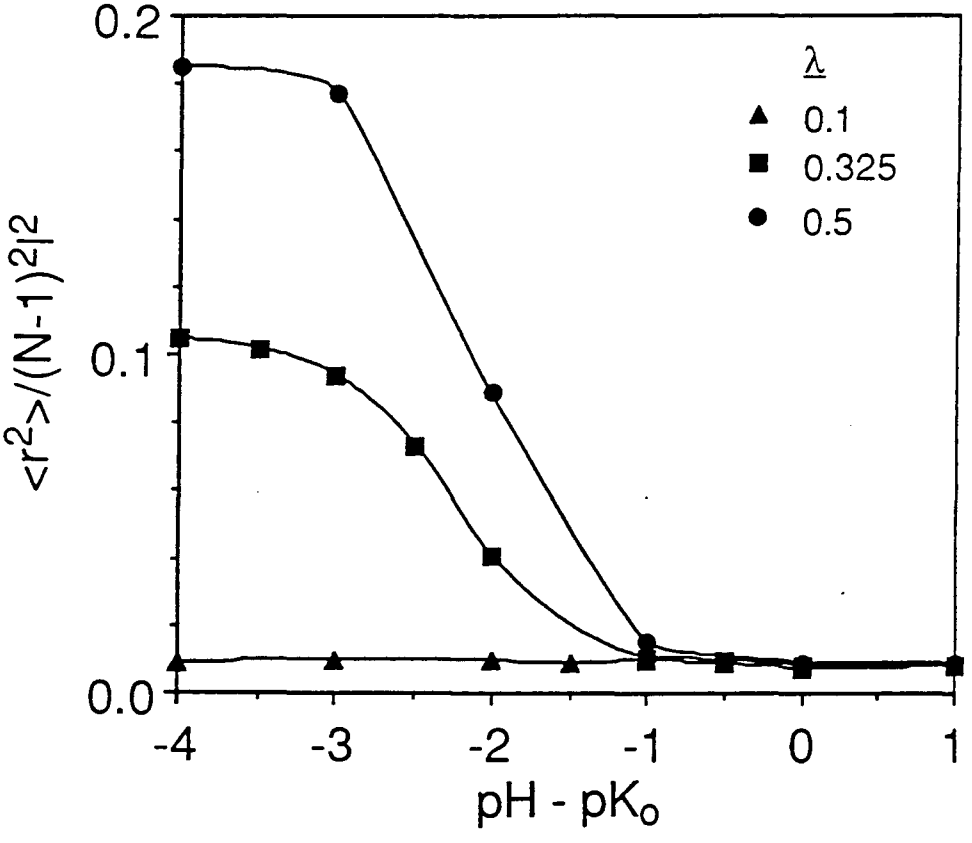

Figure 5A

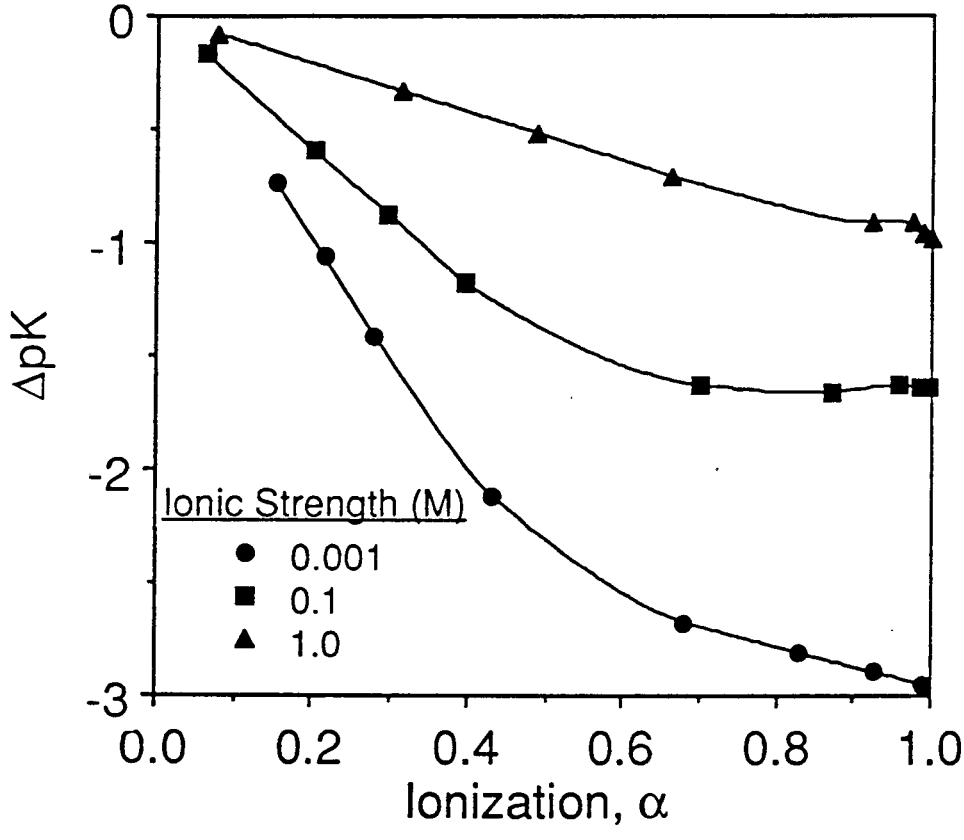
0
-1
-2
-3
ΔpK
Ionic Strength (M)
0.001
0.1
1.0
0.0
0.2
0.4
0.6
0.8
1.0
Ionization, α

Figure 5B

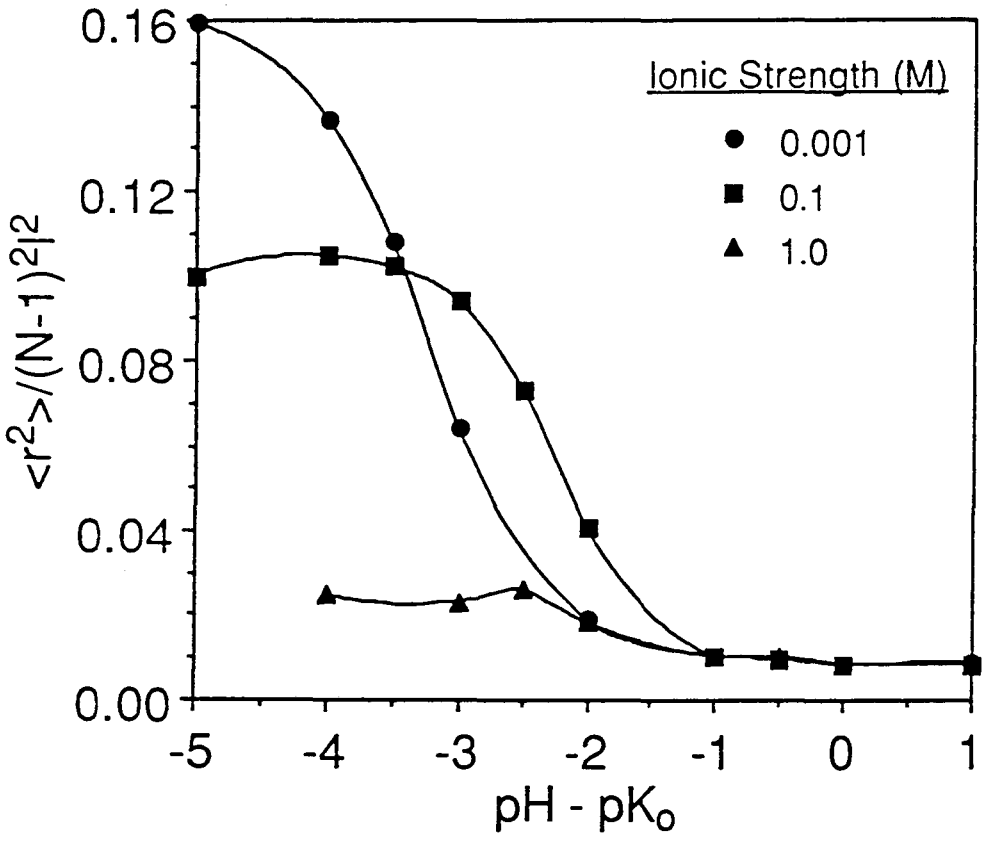
0.16
0.12
0.08
0.04
0.00
-5
-4
-3
-2
-1
0
1
$\langle r^2 \rangle / (N-1)^{2/2}$
pH - pK_o
Ionic Strength (M)
0.001
0.1
1.0

Figure 6A

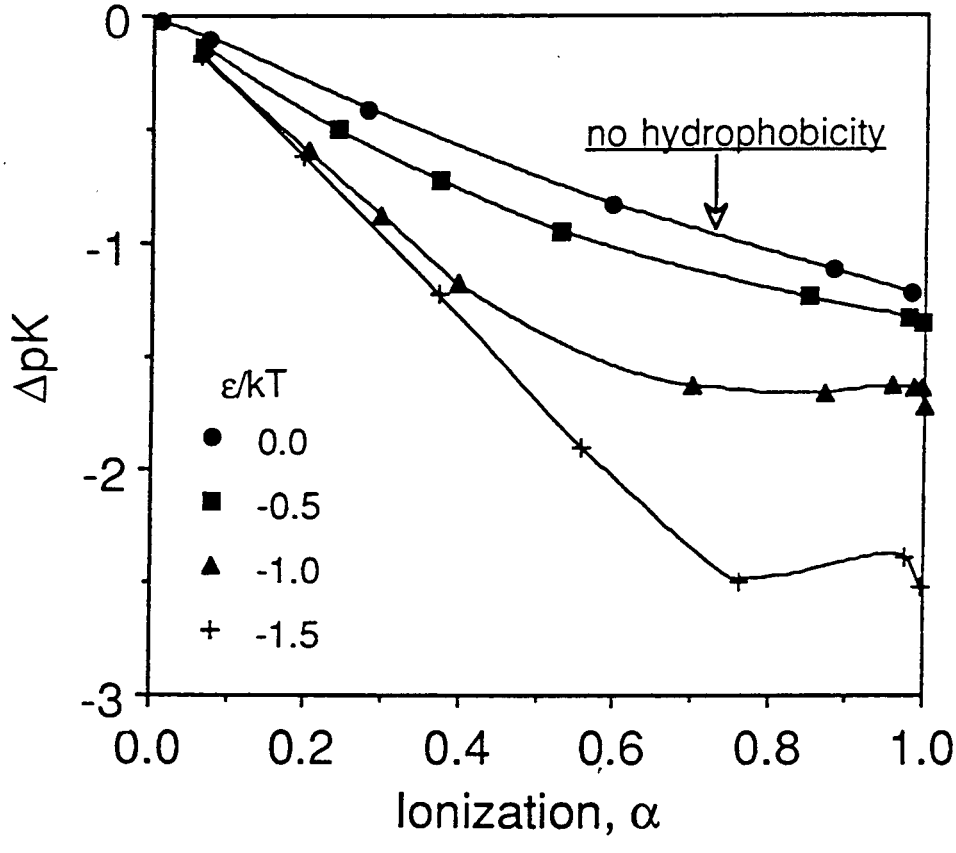
0
-1
-2
-3
ΔpK
no hydrophobicity
ε/kT
0.0
-0.5
-1.0
-1.5
0.0
0.2
0.4
0.6
0.8
1.0
Ionization, α

Figure 6B

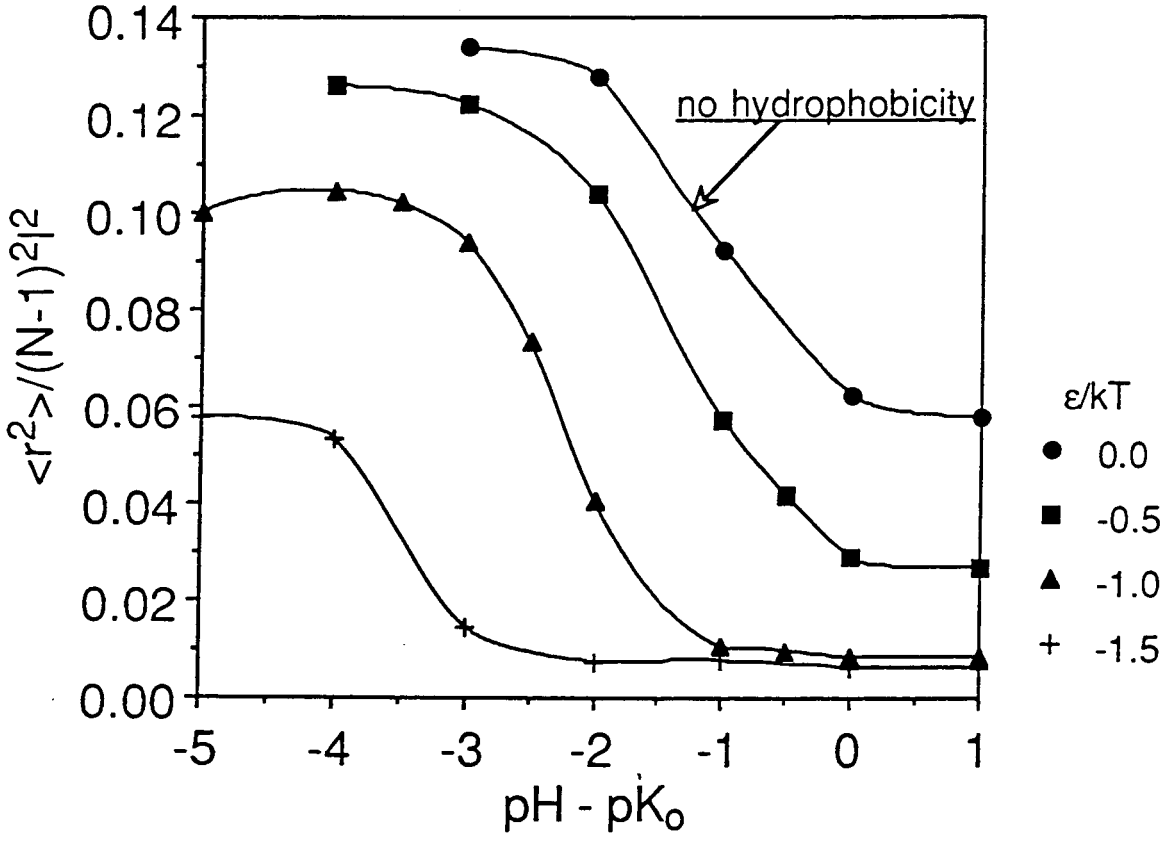
0.14
0.12
0.10
0.08
0.06
0.04
0.02
0.00
-5
-4
-3
-2
-1
0
1
$\langle r^2 \rangle / (N-1)^{2/2}$
pH - pK$_o$
no hydrophobicity
ε/kT
0.0
-0.5
-1.0
-1.5

Figure 7

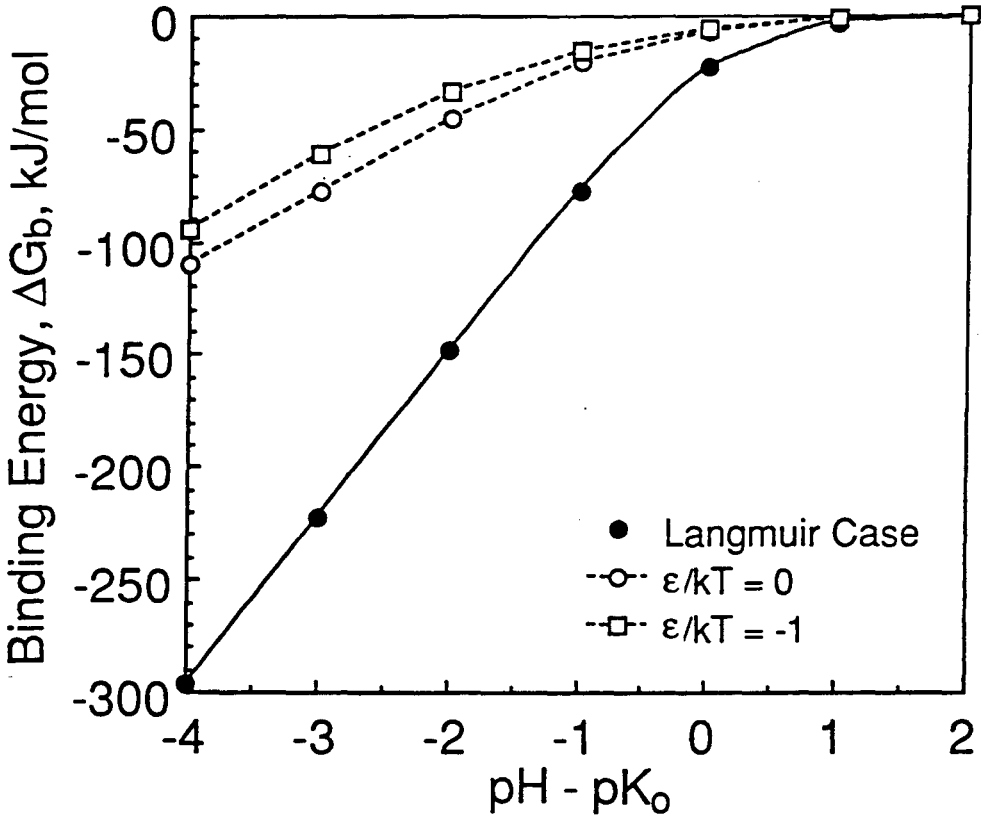
Binding Energy, ΔGb, kJ/mol
0
-50
-100
-150
-200
-250
-300
-4
-3
-2
-1
0
1
2
pH - pKo
Langmuir Case
ε/kT = 0
ε/kT = -1

LAWRENCE BERKELEY LABORATORY
UNIVERSITY OF CALIFORNIA
TECHNICAL INFORMATION DEPARTMENT
BERKELEY, CALIFORNIA 94720